Proceedings of the ASME 2025
International Mechanical Engineering Congress and Exposition
IMECE2025
November 16-20, 2025, Memphis, TN

IMECE2025-167257

ENHANCING UPPER LIMB REHABILITATION WITH FNIRS-MEASURED BRAIN ACTIVITY AND HUMAN ROBOT INTERACTION

Haider Allawi[1], Tyler Yee[1], Emily Wang[1], Justin Catalano[2], Zachariah Holder [3]Daniel Sam [3]Yue Luo[2], Yi Yuan[4], Megan Chang[5], Armin Moghadam[6], Lin Jiang[1,*]

[1]Department of Mechanical Engineering, San José State University, San José, CA
[2]Department of Industrial & System Engineering, San José State University, San José, CA
[3]Department of Biomedical Engineering, San José State University, San José, CA
[4]Department of Audiology, San José State University, San José, CA
[5]Department of Occupational Therapy, San José State University, San José, CA
[6]Department of Engineering Technology, San José State University, San José, CA

ABSTRACT

Robotics and machine learning algorithms can potentially enhance upper limb rehabilitation, addressing the limitations of traditional therapy methods. This study presents a novel Human-Robot Interaction (HRI) platform with human brain activities assessment capability aimed at enhancing upper limb rehabilitation by addressing the limitations of conventional therapy. Utilizing a 7-DOF Franka Emika robotic arm, the system supports patients in performing lifting, grasping and reaching tasks structured based on Wolf Motor Function Test (WMFT). Functional near-infrared spectroscopy (fNIRS) concurrently monitors cortical activation and functional connectivity to evaluate neural engagement and recovery. Visual feedback guides participants, while forearm EMG and brain activity from the moving limb are recorded to train deep learning models that classify physiology movement and cognitive load in real time. Quantitative performance metrics, including average trajectory deviation and non-dimensional squared jerk, assess movement accuracy and smoothness, correlating with task complexity. The platform also incorporates a robot impedance control scheme and an interactive interface to adapt assistance dynamically based on predicted movement. By integrating biomechanical performance data with neural indicators, this approach enables a personalized, data-driven rehabilitation framework.

Keywords: Robot Teleoperation, End Effector Design, fNIRS, Human Robot Interaction, Upper Limb Rehabilitation

NOMENCLATURE

n	Norm vector
q	Robot Joint Angle
T	Transformation Matrix
X	Cartesian Coordinate X axis
Y	Cartesian Coordinate Y axis
Z	Cartesian Coordinate Z axis
K	Stiffness
D	Damping
I_A	Area Moment of Inertia
τ	Joint Actuator Torque
$M(q)$	Inertia Matrix
$C(q,\dot{q})$	Coriolis and Centrifugal Matrix
$G(q)$	Gravity Matrix
$J(q)$	Geometric Jacobian Matrix
$J_v(q)$	Linear Velocity Portion of Geometric Jacobian Matrix
$J_\omega(q)$	Angular Velocity Portion of Geometric Jacobian Matrix
R_i	Coordinate Rotation Matrix
KE	Kinetic Energy
PE	Potential Energy

1. INTRODUCTION

Upper limb rehabilitation is a critical component in the recovery of individuals with motor impairments caused by stroke, traumatic injury, or neurological disorders. Traditionally, occupational therapy in clinical settings relies on therapist-guided, repetitive exercises to help individuals regain motor function. However, these conventional approaches are constrained by high therapist workloads, variability in treatment quality, and limited individual engagement [1, 2]. In response to these limitations, Human-Robot Interaction (HRI) systems and emerging technolo-

*Corresponding author: lin.jiang@sjsu.edu
Documentation for `asmeconf.cls`: Version 1.34, February 2, 2026.

gies such as machine learning and virtual reality have been explored to enhance therapy by offering consistent, data-driven, and personalized interventions [3, 4].

Rehabilitation robots can provide structured assistance ranging from passive motion, where the robot moves the patient's limb without any effort from the patient, to adaptive resistance, in which the robot adjusts resistance based on the patient's effort. Recent advancements in artificial intelligence have allowed these systems to respond dynamically to individual needs [5, 6]. Upper limb functionality becomes crucial in these cases, as rehabilitation robots must adapt to the unique needs and abilities of each individual. Traditional approaches to evaluating upper limb functionality include standardized assessments like the Wolf Motor Function Test (WMFT) and the Fugl-Meyer Assessment (FMA) [7]. More recent studies have explored sensor-based methods for quantifying motor performance, including motion capture with Kinect sensors [8, 9], electromyography [10], and functional near-infrared spectroscopy (fNIRS) [11], which offer more frequent, objective, and non-invasive monitoring.

While sensor-based methods offer significant benefits, they also present challenges, primarily the complexity of the recorded data. Machine learning models, particularly deep neural networks (DNNs), are capable of interpreting this data, predicting motion trajectories, and even estimating rehabilitation outcomes [12, 13]. These tools can reduce therapist workload while supporting more individualized recovery planning [14, 15]. In parallel, 3D visualized platforms provide immersive rehabilitation environments and can facilitate motor imagery in early-stage recovery or for individuals with limited mobility [16, 17]. When integrated, these technologies present a powerful opportunity to reshape the delivery and evaluation of rehabilitation.

This study aims to develop an integrated rehabilitation platform that leverages machine learning, functional near-infrared spectroscopy (fNIRS) [18], real-time physiological function assessment, and robotic assistance to support recovery in individuals with upper limb motor impairments. The proposed system is designed to be adaptive, scalable, and user-centered, directly addressing critical limitations in traditional therapy, such as inconsistent feedback, limited personalization, and challenges in maintaining individual engagement. At the core of the system is a machine learning model trained on fNIRS data and EMG data to assess motor functionality, using the Wolf Motor Function Test (WMFT) as a clinical benchmark. By interpreting neural activity during motor tasks, the system can classify an individual's motor function capacity and track progress over time. Based on these classifications, personalized rehabilitation trajectories are generated to reflect the individual's capabilities and therapeutic goals. These trajectories are then executed through a dexterous robotic platform that provides real-time, guided assistance. This approach ensures that individuals receive consistent, repeatable therapy while reducing the burden on clinical staff.

The system integrates neurophysiological monitoring to analyze brain activity in response to physical actions, providing insight into both functional recovery and neural adaptation. The combination of objective data verification and robot-assisted personalized training supports the development of a clinical assessment tool for upper limb rehabilitation. Ultimately, this work contributes a novel framework that enhances hospital-based occupational therapy by fusing intelligent evaluation, personalized intervention, and robotic support into a unified therapeutic system.

2. METHODOLOGY

The proposed rehabilitation system integrates machine learning, functional near-infrared spectroscopy (fNIRS), robotic assistance, and trajectory generation into a unified platform designed to support personalized upper limb therapy. The system architecture consists of three core components: (1) acquisition of brain activity data via fNIRS during motor tasks, (2) deep neural network (DNN) classification of motor functions via surface electromyography (EMG) signals, (3) impedance robot guidance.

2.1 Experimental Setup

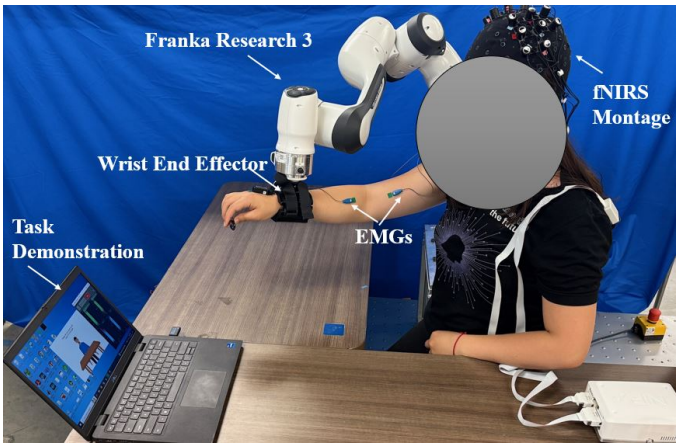

FIGURE 1: EXPERIMENTAL SETUP.

A pilot study was conducted with healthy individuals to assess the feasibility of the proposed multi-modal rehabilitation system, which integrates visual stimulation, robotic assistance, muscle activity monitoring, and neuroimaging. The experimental setup is described as in Figure 1. This pilot study involved three healthy adult participants (two male, one female; ages 19, 25, and 35 years), all right-hand dominant with no history of neurological or musculoskeletal disorders. All participants completed the full sequence of upper limb tasks in both unassisted and robot-assisted conditions. The study was approved by the Institutional Review Board (IRB) of San José State University IRB 24-286), and informed consent was obtained from all participants prior to data collection.

The task set, as demonstrated in Figure 2, included: Place your forearm on the desk (Task 1), Place your forearm on the box (Task 2), Move your forearm with weight (Task 3), Pick up a can (Task 4), and Pick up a pen (Task 5). These tasks were not randomized as the WMFT is a sequential evaluation of motor functions. The participants were shown all the tasks they would perform, with the moderator confirming their understanding. The experiment flowed as follows: video instructions (5 seconds), text instructions (5 seconds), onset of the "start movement" marker (5 seconds), jitter (randomly 8, 10, or 12 seconds), then reset (5 seconds). Each task is to be performed five times, including

times of instructions, onset, jitter (holding of the position), and reset, before moving on to the next task.

While completing tasks with and without robotic assistance (2.3), sensors including an fNIRS montage (2.2), electromyography (EMG) (2.4), and inertial measurement units (IMUs) (2.4) were attached to participants to capture neural activity, muscle engagement, and movement trajectories. This data was then fed into machine learning models to predict effort levels and task performance.

2.2 fNIRS montage and experimental setup

To deliver task instructions and synchronize neurophysiological recordings with motor activity, a custom visual stimulation protocol was developed using PsychoPy (version 2025.1.1). The program was designed to present a sequence of five 2D animated motor function tasks modeled after the Wolf Motor Function Test (WMFT), a standardized assessment used to evaluate upper limb function. Each animation visually demonstrated the movement to be performed by the participant and served both as a cognitive cue and motor planning stimulus.

Synchronization with fNIRS data acquisition and EMG logging was achieved through digital event triggers. PsychoPy was configured to send serial port triggers via local ethernet at the onset of each animation and at movement execution cues, enabling precise alignment of neurophysiological data with stimulus timing, as presented in Figure 3. This trigger-based system ensured that brain and muscle activity could be reliably segmented and analyzed in correspondence with specific tasks.

All visual stimuli were presented on a 24-inch LCD monitor placed approximately 60 cm from the participant's seated position. Participants were instructed to follow each animated movement using their right hand.

This setup provided a repeatable and controlled method of presenting task cues, while enabling synchronized data collection for analyzing cortical and muscular responses across standardized upper limb rehabilitation tasks.

2.3 Robot-assisted Upper Limb Guided Physical Training

Robot-assisted training was delivered using a 7-DoF Franka Emika Research 3 (FR3) robot, controlled via an impedance-based interaction scheme [19]. The 7-degree-of-freedom Franka Emika Research 3 (FR3) robot was selected for this study due to its built-in torque sensors, high-resolution joint control, and native support for impedance-based interaction. These features make it particularly well-suited for upper limb rehabilitation tasks that require compliant, adaptive movement in response to human interaction. The robot's redundancy allows for flexible arm configurations during therapy, and its real-time ROS-compatible control interface enabled the integration of multimodal physiological feedback for adaptive guidance. Compared to other commercially available platforms, the FR3 offered an optimal balance between safety, responsiveness, and programmability in a research-focused rehabilitation setting. The system enables assisted and guided physical therapy through impedance-controlled, trajectory-based movement generation that aligns with the Wolf Motor Function Test (WMFT) designed in Section 1.

The dynamic behavior of the FR3 robot is modeled using Lagrangian mechanics. The equations of motion for both the lead (l) and follower (f) robots in joint space are described as:

$$\tau_l + \tau_h = M_l(q_l)\ddot{q}_l + C_l(q_l, \dot{q}_l)\dot{q}_l + G_l(q_l) \tag{1}$$

$$\tau_f + J(q_f)^T F_{ext} = M_f(q_f)\ddot{q}_f + C_f(q_f, \dot{q}_f)\dot{q}_f + G_f(q_f) \tag{2}$$

Here, q_l and q_f represent joint positions; M, C, and G correspond to the inertia matrix, Coriolis/centrifugal forces, and gravity vector, respectively. $J(q_f)^T F_{ext}$ captures the external force applied at the end-effector.

The robot's kinetic energy is defined as:

$$KE = \frac{1}{2}\dot{q}^T M(q)\dot{q} \tag{3}$$

where $M(q)$ is the mass matrix derived as:

$$M(q) = \sum_{i=1}^{n} \left[m_i J_{v_i}(q)^T J_{v_i}(q) + J_{\omega_i}(q)^T R_i(q) I_i R_i(q)^T J_{\omega_i}(q) \right] \tag{4}$$

The system's potential energy is given by:

$$PE = \sum_{i=1}^{n} g^T r_{ci} m_i \tag{5}$$

where g is the gravitational vector, and r_{ci} is the position of the center of mass of link i.

An impedance controller governs the interaction between robot and participant. The control input is defined as:

$$\tau = \hat{M}(q)\ddot{q}_d + C(q, \dot{q})\dot{q} + G(q) + D(\dot{q}_d - \dot{q}) + K(q_d - q) \tag{6}$$

Assuming perfect model estimation ($\hat{M}(q) = M(q)$), the closed-loop dynamics simplify to:

$$\tau_h = M_{m,l}(q_l)(\ddot{q}_{d,l} - \ddot{q}l) + D_l(\dot{q}d, l - \dot{q}l) + K_l(qd, l - q_l) \tag{7}$$

$$\tau_{ext} = M_{m,f}(q_f)(\ddot{q}_{d,f} - \ddot{q}f) + D_f(\dot{q}d, f - \dot{q}f) + K_f(qd, f - q_f) \tag{8}$$

The robot's interaction with the participant was regulated by an impedance controller (Figure 4) that follows participant's trajectories. Feedback on joint positions, torques, and end-effector forces was collected in real time using OPC UA. Workspace mapping ensured consistent motion scaling between input and output configurations, using the following linear transformation:

$$Y = (X - X_{min}) \times \left(\frac{Y_{max} - Y_{min}}{X_{max} - X_{min}} \right) + Y_{min} \tag{9}$$

TABLE 1: PARTICIPANT DEMOGRAPHIC AND EXPERIMENTAL INFORMATION

Participant ID	Sex	Age (years)	Dominant Hand	Notes
1	Male	19	Right	No reported neurological issues
2	Male	25	Right	No reported neurological issues
3	Female	35	Right	No reported neurological issues

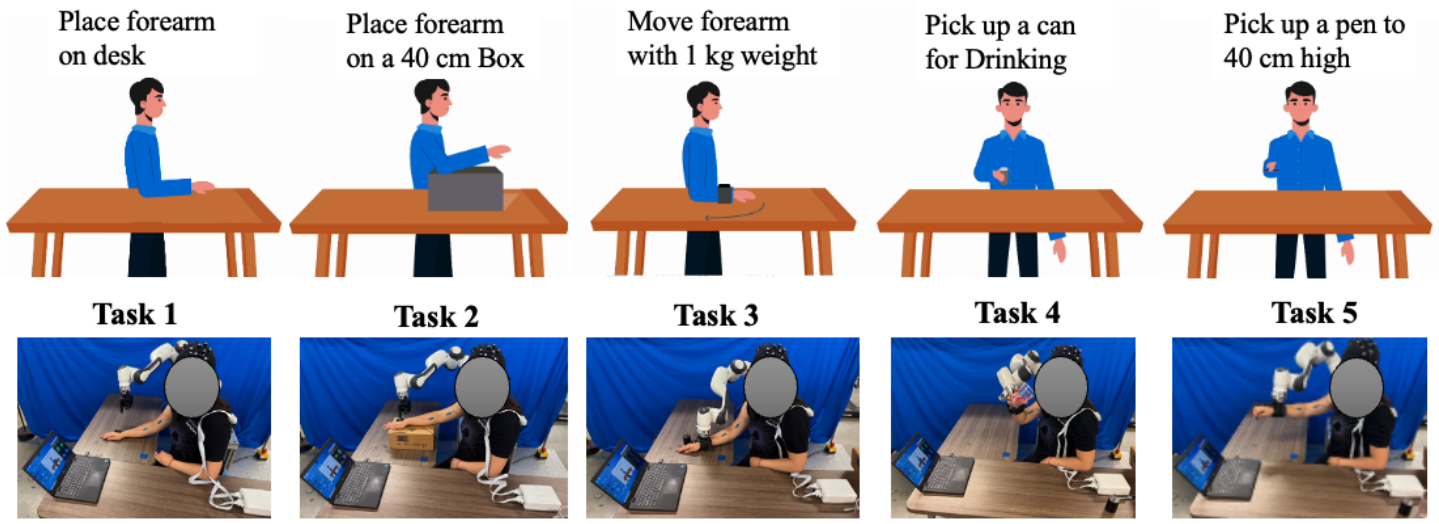

FIGURE 2: FNIRS EXPERIMENTAL DESIGN WITH PSYCHOPY INTEGRATION

The control architecture, implemented in Simulink, is shown in Figure 4. The model managed real-time impedance adjustments based on user interaction, supporting smooth and responsive guidance throughout the tasks.

Only one set of impedance parameters was implemented for the robot-assisted tasks. This configuration was informed by neurophysiological findings from fNIRS and EMG data classification, which highlighted the need to balance participant engagement with safety and motion fidelity. Cortical activation and muscle recruitment observed during active task conditions allow us to consider high, moderate, or low impedance for promoting neuromuscular involvement without overloading the participant. The example of a set of selected joint-level stiffness (K) and damping (D) gains [6] for wrist support is presented in Table 2.

TABLE 2: IMPEDANCE GAINS SETUP IN ROBOT-ASSISTED MODE

Gain Type	Joint						
	q_1	q_2	q_3	q_4	q_5	q_6	q_7
Stiffness (K)	800	800	800	800	500	300	100
Damping (D)	50	50	50	50	30	25	15

This impedance configuration was used exclusively during robot-assisted trials to provide real-time, compliant motion assistance based on the individual's effort and interaction forces. In contrast, unassisted tasks were performed without robotic intervention, serving as a baseline for comparison. By integrating classified tasks and biomechanical response, the impedance controller ensured smooth, safe, and adaptive physical interaction during assisted and guided rehabilitation exercises.

The custom-designed wrist-mounted end effector (Figure 5) was developed to provide stable and secure forearm support during robot-assisted rehabilitation. Its modular and ergonomic design accommodates individuals with muscle stiffness, weakness, or limited voluntary control, ensuring safe and effective transfer of actuation forces from the robot to the participant's limb. Following modular design principles described in [6], the end effector supports ambidextrous mounting and allows for customizable adjustments based on forearm size and posture. Additionally, the system can be extended with interchangeable elbow and shoulder adapters, enabling targeted stabilization and assistance at different anatomical locations to accommodate diverse therapeutic needs.

2.4 Electromyography (EMG) Sensor Setup and Muscle Engagement

To assess muscle engagement during both unassisted and robot-assisted upper limb tasks, surface electromyography (EMG) sensors were used to capture activity from four primary muscles: Biceps Brachii (BB), Triceps Brachii (TB), Flexor Carpi Radialis (FCR), and Flexor Digitorum Superficialis (FDSF). These muscles are frequently activated during occupational therapy tasks such as reaching, grasping, and lifting. An additional inertial measurement unit (IMU) was placed on the extensor digitorum to record wrist orientation and movement. Figure 6 illustrates sensor placement on the participant's dominant limb.

Participants first performed a task series of task 1, task 2, task 3, task 4, and task 5 that were unassisted, which served as a baseline. Each task was performed under two engagement levels: unassisted mode, involving normal muscle activation without assistance, and an assisted mode, in which participants' wrist, elbow or shoulder joint are connected to FR3 robot using specific

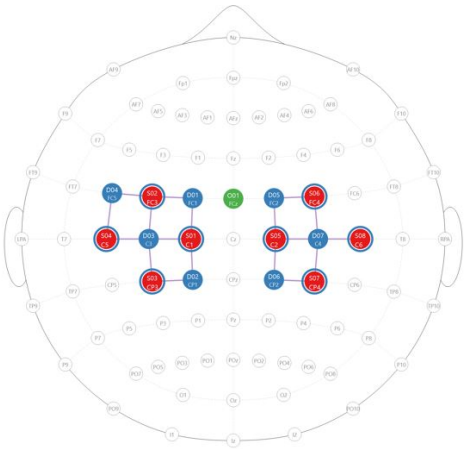

(a)

(b)

FIGURE 3: (A) FNIRS MONTAGE DESIGN AND (B) SOURCE AND DETECTOR PLACEMENT

end effector adapter during the motion to simulate muscular resistance.

Following the unassisted trials, participants repeated the task sequence using robot-assisted movement, guided by the Franka Emika Research 3 (FR3) robot. While seated, participants were connected to a custom wrist-mounted end effector. In the Relaxed condition, they followed the robot's motion passively with minimal grip or resistance. In the Resisting condition, participants actively opposed the robot's movement in the z-direction, simulating active participation and effort during therapy.

EMG signals were acquired using the Delsys EMGworks system and processed in EMGworks Analysis. Signals were normalized to each muscle's maximum voluntary contraction (MVC) using root mean square (RMS) values. A Butterworth filter was applied to reduce noise, while IMU data were filtered using an inclination filter to isolate relevant kinematic features.

To estimate human-applied force and muscle effort, a least mean squares (LMS) filter was used. The resulting clean signals were integrated into a hybrid model that included a deep neural network (DNN) trained on both EMG and IMU features. This model classifies and predict the tasks being performed, enabling real-time adaptation during therapy and post-analysis of individual engagement and functional capacity.

3. RESULTS AND DISCUSSION

3.1 fNIRS-Based Neural Activity Trends

Figure 7 show the measures from fNIRS: mean oxygenated (HbO) and deoxygenated (HbR) hemoglobin concentrations. An increase in HbO typically reflects higher neural activity in a brain region. A decrease in HbR is often observed alongside an increase in HbO during neural activation. HbO increased significantly over channels corresponding to the left motor cortex, aligning with right-arm movement during the task. Among all figures, the first peak indicates the start of the task, and the second peak indicates the holding portion of the task. The averages are calculated after dropping channels with low coupling index, indicating that the data from them is pure noise. The mean was then calculated for all channels across the five repetitions of a task.

To ensure data quality, the averages were calculated after excluding channels with a low coupling index—defined as those with a correlation coefficient below 0.75 between the two wavelengths (760 nm and 850 nm) used in optical density measurements. This threshold is commonly used in fNIRS [20] to detect channels affected by poor optode contact or motion artifacts. On average, 10–15% of channels were removed per participant. These channels were considered to contribute primarily noise rather than meaningful neural signals, and their exclusion improves the reliability of the calculated hemodynamic response.

The mean was then calculated for all remaining channels across the five repetitions of a task. The rapid increase of HbO following the task onset was most pronounced over channels covering the contralateral primary motor cortex (M1), consistent with activation during right upper limb movement. Additional activation in prefrontal regions during Tasks 2 and 5 suggests heightened cognitive engagement during these more complex or goal-oriented movements. The HbR has a reduced response during brain activity, which may indicate that the rate of oxygen delivery outpaces the consumption of oxygen by the cells. Toward the end of the task, the concentrations return toward the baseline.

Figure 7e most clearly depicts the concentration responses from the starting and holding portions of the task. Each peak is clear and distinct, showing a directly observable difference in engagement throughout the task. A tertiary peak is also visible, indicating a further change in cognitive engagement beyond the two phases of the task. Figure 7b similarly depicts a clean response. The overall larger magnitude compared to the others tasks indicates a higher level of cognitive engagement needed by the task. Figure 7c contains four distinct peaks indicating further sources of cognitive engagement beyond the two phases of the task. Figure 7d shows a less distinguishable graph. The holding peak still occurs, however, at a greatly reduced magnitude, showing minimal deviation from baseline noise. The reduced peak indicates that the hold phase required much lower cognitive engagement to perform. A tertiary peak then indicates a further stimulus. Finally, Figure 7e contains clear and distinct peaks for the two phases of the task, followed by a tertiary peak indicating a change in stimulus.

One cause of the tertiary and quaternary peaks is that reset movements are likely being captured as tertiary peaks. For example, in task 5, the pencil needs to be returned to the table. The

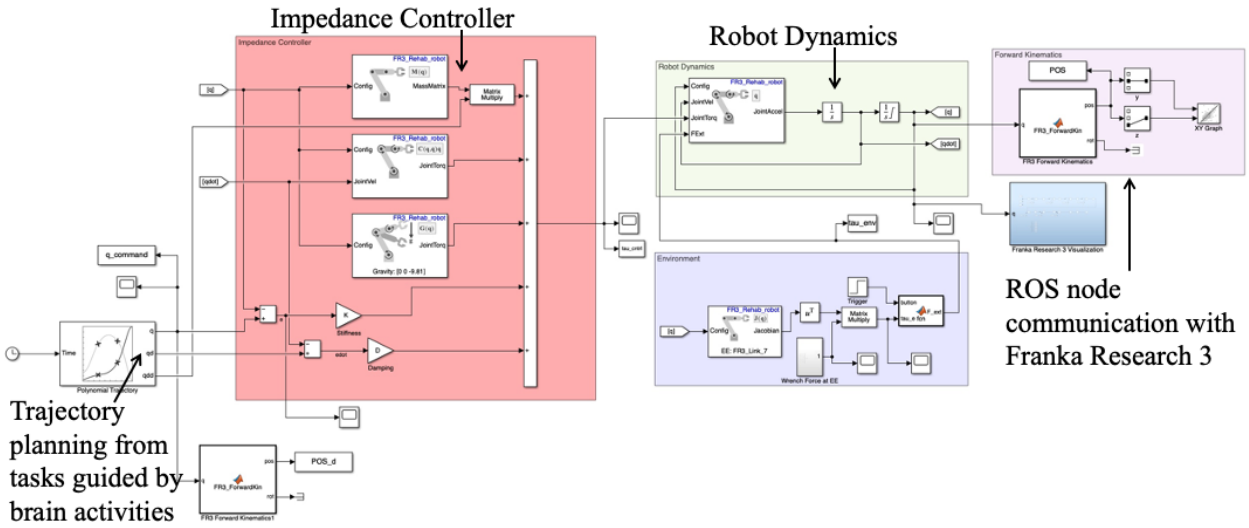

FIGURE 4: SIMULINK MODEL FOR JOINT IMPEDANCE CONTROL OF THE FR3 ROBOT

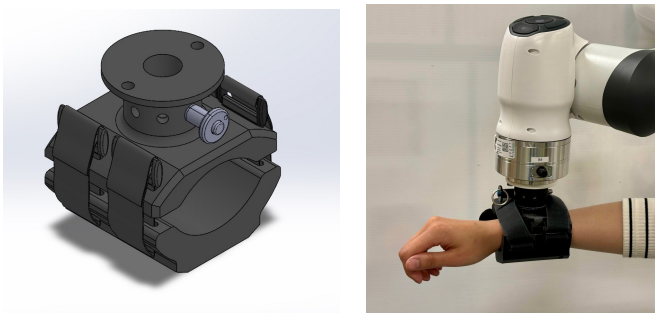

(a) (b)

FIGURE 5: CUSTOM WRIST-MOUNTED END EFFECTOR FOR FRANKS EMIKA RESEARCH 3 ROBOT (FR3)

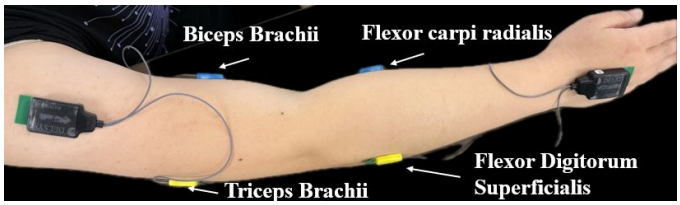

FIGURE 6: EMG SENSOR PLACEMENT ON RIGHT UPPER LIMB

movement for this requires cognitive engagement, lowering the arm, releasing the fingers, and stopping the pencil from moving. All of this leads to the presence of additional peaks. Another cause of additional peaks and fluctuations during a task is because of distractions, sudden noises, making additional motions than described in the task, and visual distractions all contribute towards the conative engagement of a subject.

3.2 Using DNN to Predict and Classify Tasks via Muscle Activation Measurement from EMG

The convolutional neural network (three 1-D convolutional layers followed by two fully connected layers) achieved a validation accuracy of 81.97% after convergence (Figure 8). Overall confusion matrix is also presented in Figure 8. Although lower than the preliminary expectation reported earlier, the model still performed well given the modest dataset size and pared-down architecture. Validation loss stabilized after 25 epochs, indicating limited over-fitting once early stopping was triggered.

TABLE 3: TASK-LEVEL CLASSIFICATION PERFORMANCE

Task ID	Action performed	Precision %
1	Place forearm on desk	71%
2	Place forearm on a 40 cm high box	19%
3	Move forearm with 1kg weight	67%
4	Pick up can to mouth for drinking	56%
5	Pick up a pen to 40cm high	48%

Table 3 shows detailed results of the classification. We observed High performers (Tasks 1 & 3, Place arm on the table, and Move forearm with weight correspondingly) and low performer (Task 4, Pick up a can to mouth for drinking). Both actions involve distinctive flexor/extensor activation with limited overlap, enabling reliable separation. The EMG signature of a cylindrical grasp overlaps those of lighter pen lifts (Task 5) and weighted movements (Task 3), leading to misclassifications. Denser electrode coverage of intrinsic hand muscles or additional kinematic channels could improve discrimination. Moderate confusion (Tasks 2, Place arm on a 40 cm box) shared shoulder–elbow trajectories with Task 4 and Task 5, which blurs boundaries, adding inertial-measurement-unit (IMU) data or spatially richer EMG maps may help.

These observations also highlight the inherent limitations of relying solely on surface EMG signals. EMG-based classification can be challenged by cross-talk between adjacent muscles, individual variability in muscle recruitment, and overlapping activation patterns in complex tasks. To address these challenges, we recognize the value of multi-sensor fusion. Future work will explore combining EMG with complementary modalities such as IMUs for 3D kinematics, which can help distinguish tasks with

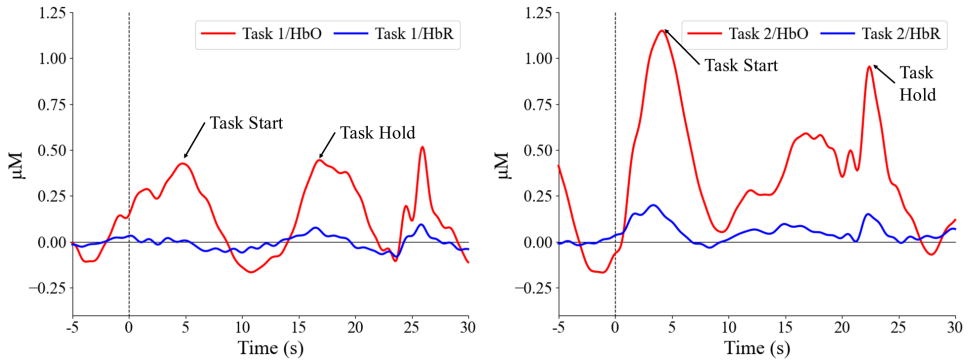

(a) Task 1: Place forearm on the desk

(b) Task 2: Place forearm on a 40 cm box

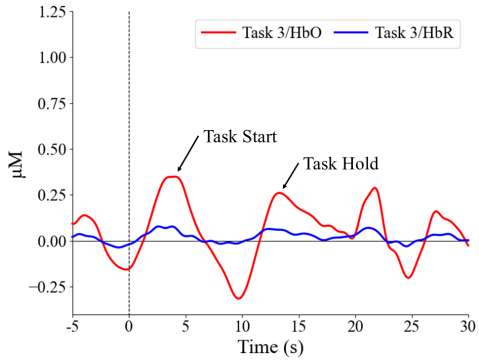

(c) Task 3: Move forearm with 1 kg weight

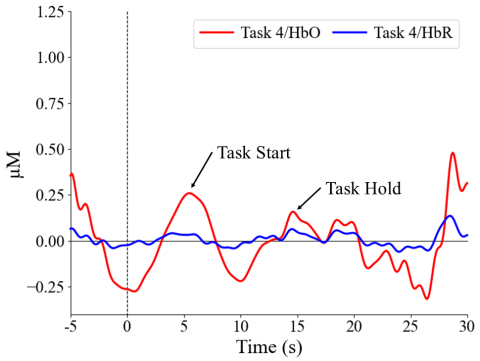

(d) Task 4: Pick up can to mouth for drinking

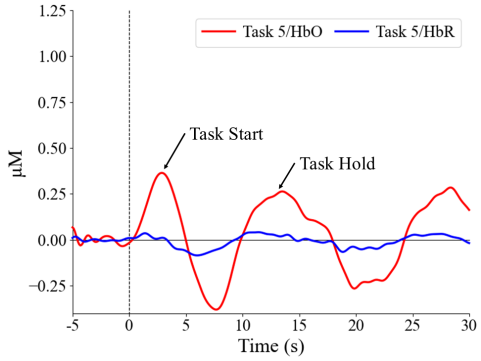

(e) Task 5: Pick up a pen to 40 cm high

FIGURE 7: MEAN CONCENTRATION OF OXYGENATED (HBO) AND DEOXYGENATED (HBR) HEMOGLOBIN ACROSS ALL TASKS. CALCULATED FROM ALL SOURCE-DETECTOR PAIRS ACROSS ALL TRIALS WITHIN A GIVEN TASK.

similar muscle activations but different spatial trajectories. Additionally, increasing the number of EMG channels to include finer-grained muscle groups—particularly in the hand and shoulder—can enhance task separability and robustness of the classification pipeline.

The notably lower precision scores for Task 2 (19%), Task 4 (56%) and Task 5 (48%) need further analysis. Task 2 is placing the forearm on a 40 cm high box, which involves a lifting motion that shares joint trajectories and muscle engagement patterns with other vertical reaching tasks (Tasks 4 and 5), leading to overlapping EMG signals. Similarly, Task 4 (picking up a can to the mouth for drinking) requires a compound movement involving shoulder flexion, elbow flexion, and wrist stabilization. These muscle activations overlap with both weighted movements (Task 3) and lighter object manipulations (Task 5), which likely contributed to classification ambiguity. These lower scores may reflect not only the complexity and similarity of the biomechanical profiles involved but also limitations in the current sensor configuration and model granularity. In particular, the limited EMG electrode coverage of intrinsic hand muscles and absence of hand kinematics likely reduced the model's ability to discriminate fine-grained motor patterns.

Comparative analysis with similar studies shows consistent trends. For instance, prior work by Zhou et al. [21] and Kim et al. [22] also report reduced classification accuracy in tasks involving fine object manipulation or compound movements with overlapping activation profiles. These studies highlight the importance of multimodal inputs (e.g., combining EMG with IMU

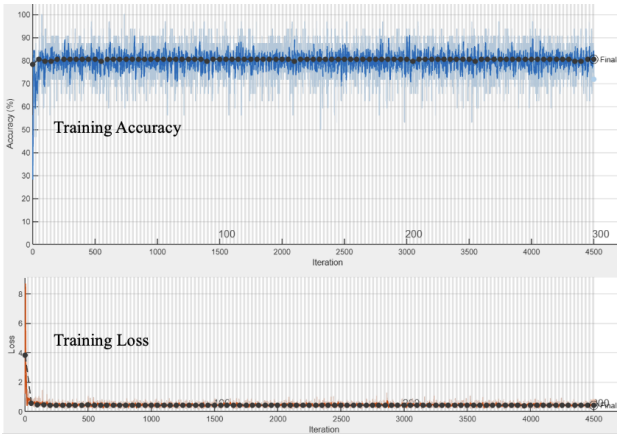

(a) Training Accuracy and Loss

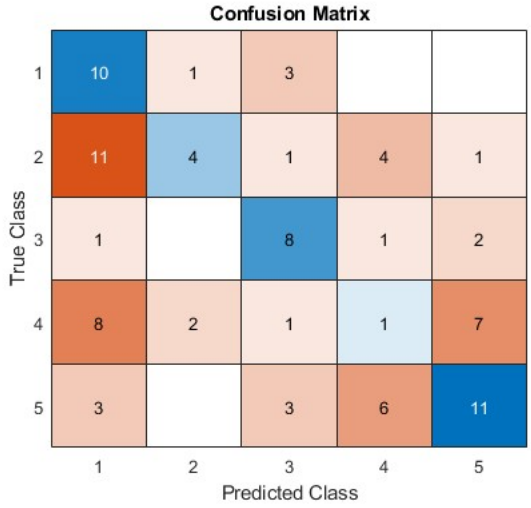

(b) Confusion Matrix

FIGURE 8: DNN MACHINE LEARNING FOR CLASSIFY TASKS WITH PARTICIPANTS

or vision-based tracking) to improve discriminability across similar functional tasks. As future work, we plan to increase EMG spatial resolution, incorporate inertial sensing, and expand the dataset size to support more robust, task-specific classification. This will allow the system to better distinguish nuanced movements and support clinical deployment for a wider range of rehabilitation scenarios.

The task-specific classification accuracies highlight where the current EMG-driven control pipeline is ready for clinical deployment (gross placement and resisted forearm movement) and where further signal enhancement is required (power grasp and intermediate elevations). These insights provide a quantitative road map for refining sensor placement and multimodal fusion to achieve truly adaptive, intention-aware rehabilitation robotics.

3.3 Neurophysiological Insights and Impedance Stiffness Recommendation for Training

Integrated analysis of fNIRS and EMG signals provided valuable insight into participant effort, engagement levels, and neural activation under different training conditions. This data was used to inform recommendations for selecting appropriate impedance stiffness values in upper limb rehabilitation scenarios.

fNIRS measurements revealed increased cortical activation—specifically elevated oxygenated hemoglobin (HbO) levels—in both motor and prefrontal regions during five tasks across robot-assisted and unassisted modes. It suggests higher cognitive and motor effort when individuals actively engage with robots in movement control. EMG signals confirmed this pattern, showing increased average values for all four monitored muscles during Task trials, particularly the Biceps Brachii and Flexor Carpi Radialis.

Based on this individual's data, a light impedance stiffness profile is recommended for upper limb rehabilitation tasks designed to elicit active user participation while maintaining safety. Specifically, joint stiffness values in the range of:

- K = [300–500] N·m/rad for shoulder and elbow joints (q_1–q_4),
- K = [150–300] N·m/rad for wrist joints (q_5–q_6),
- $K \leq 100$ N·m/rad for distal joints (q_7),

were found to encourage meaningful muscular engagement without overloading the participant, especially during robot-assisted modes. These values balance the need for support with the goal of maintaining high neural activation, as supported by the combined fNIRS and EMG responses.

While only a single set of impedance parameters was applied in the current study, the observed task-dependent variations in neural and muscular engagement highlight the potential of dynamic impedance tuning. In future work, we aim to implement an adaptive control framework in which impedance parameters are adjusted in real time based on physiological indicators—particularly fNIRS-derived cognitive load and EMG-based effort metrics. For example, sustained increases in HbO within prefrontal or motor cortex regions could indicate heightened cognitive load or task difficulty, prompting a decrease in stiffness to reduce user burden. Conversely, low neural engagement could trigger an increase in challenge through greater resistance or task complexity. This strategy aligns with emerging research in real-time, intention-aware HRI systems. Previous study from the authors [6] demonstrated the integration of motion intention detection into impedance control for upper extremity disorders, while Zhao et al. [23, 24] proposed a shared control paradigm using intention estimation to adjust robotic assistance levels dynamically. These studies support the feasibility and effectiveness of adaptive impedance control driven by physiological and cognitive cues, particularly in rehabilitation robotics.

Integrating fNIRS and EMG within such a control loop would enable personalized therapy tailored to the user's moment-to-moment state, ultimately improving both engagement and outcomes. This multimodal fusion approach represents a promising next step toward fully responsive, intelligent rehabilitation systems.

3.4 User Engagement and Future Clinical Validation

While fNIRS and EMG data provided valuable insight into neural and muscular engagement during rehabilitation tasks, the

current pilot study did not include subjective engagement metrics or behavioral feedback. Nonetheless, participant motivation and sustained cognitive focus are essential for the effectiveness of repetitive rehabilitation protocols. To support these goals, we plan to develop a gamified interaction interface aimed at improving user engagement throughout therapy sessions.

The proposed gamified layer will feature real-time visual feedback, performance-based progress tracking, and adaptive task challenges that respond to the participant's physiological signals and motion accuracy. By transforming standard rehabilitation exercises into interactive, goal-driven experiences, we aim to create a more immersive and motivating environment. Prior studies [25–27] have demonstrated that such gamification strategies can enhance adherence and treatment outcomes, especially in long-term or home-based rehabilitation contexts.

In parallel, we are preparing a follow-up clinical study involving stroke patients with upper limb motor impairments. This trial will evaluate the safety, usability, and therapeutic potential of the system in a clinical setting. Conducted under IRB-approved protocols, the study will include multiple therapy sessions per participant and assess both functional outcomes—such as the Fugl-Meyer Assessment (FMA) and the Wolf Motor Function Test (WMFT)—and subjective engagement metrics. Physiological signals will be continuously monitored to assess cognitive and motor workload across sessions. These next steps will provide the necessary validation to generalize the platform to clinical populations and support its advancement toward intention-aware, adaptive neurorehabilitation.

This study serves as an initial pilot and is, to our knowledge, the first to integrate real-time fNIRS-based cortical monitoring with EMG-driven robotic assistance for upper limb therapy. The primary objective was to investigate whether meaningful relationships exist between motor performance and brain activity during structured tasks. The results provide early evidence that neural activation patterns may offer actionable input for adaptive impedance control, enabling task difficulty and robotic assistance to be dynamically tuned based on user cognitive load.

We acknowledge several limitations, including the small sample size of three healthy individuals and the absence of a formal step-by-step clinical therapy protocol. These constraints limit the generalizability of our current findings. Future work will focus on recruiting a broader and more diverse participant pool, including stroke survivors; integrating additional sensing modalities such as inertial measurement units (IMUs), higher-resolution EMG arrays, and hand kinematics; and establishing a clinically informed, progressive rehabilitation protocol. These efforts will lay the groundwork for deploying an adaptive, patient-centered neurorehabilitation platform in real-world therapeutic settings.

4. CONCLUSION

This study presents a novel, integrated rehabilitation platform that combines robot-assisted therapy, machine learning, and real-time neurophysiological monitoring to support upper limb motor recovery. The system utilizes a 7-DOF Franka Emika robot to deliver impedance-controlled physical assistance for tasks modeled on the Wolf Motor Function Test (WMFT), while functional near-infrared spectroscopy (fNIRS) and surface electromyography (EMG) capture brain and muscle activity. A deep neural network was trained to classify motor engagement across tasks using multimodal input, providing real-time insights into participant effort and functional capacity. To our knowledge, this is the first study to systematically examine cortical hemodynamics during guided upper limb rehabilitation, establishing a direct link movement and neurocognitive activation. This approach enables adaptive, personalized therapy through data-driven modulation of impedance parameters based on individual engagement. Limitations include the use of a healthy cohort, small sample size, and reduced classification accuracy in tasks involving complex or overlapping motions. Future work will expand to clinical populations, incorporate richer sensor arrays for fine-grained intention detection, and explore closed-loop control based on real-time brain activity. By integrating biomechanics with brain monitoring, this platform lays the groundwork for intelligent, intention-aware neurorehabilitation.

ACKNOWLEDGMENTS

This work was supported by the National Science Foundation (NSF) under Directorate for Computer and Information Science and Engineering (CISE), Award No. 2431636. The authors would also like to thank Jonathan Lim for his assistance with 3D printing services, which contributed significantly to the development of the experimental setup.

REFERENCES

[1] Donnelly, C., Leclair, L., Hand, C., Wener, P., and Letts, L., 2023. "Occupational therapy services in primary care: a scoping review". *Primary Health Care Research & Development,* **24**, p. e7.

[2] Wressle, E., and Samuelsson, K., 2014. "High job demands and lack of time: A future challenge in occupational therapy". *Scandinavian Journal of Occupational Therapy,* **21**(6), pp. 421–428.

[3] Hong, R., Li, B., Bao, Y., Liu, L., and Jin, L., 2024. "Therapeutic robots for post-stroke rehabilitation". *Medical Review,* **4**(1), pp. 55–67.

[4] Khalid, U. B., Naeem, M., Stasolla, F., Syed, M. H., Abbas, M., and Coronato, A., 2024. "Impact of ai-powered solutions in the rehabilitation process: Recent improvements and future trends". *International Journal of General Medicine,* **17**, pp. 943–969.

[5] Mohebbi, A., 2020. "Human-robot interaction in rehabilitation and assistance: a review". *Current Robotics Reports,* **1**(3), pp. 131–144.

[6] Banzon, A. J., Wang, E., Luo, Y., Jin, L., and Jiang, L., 2025. "Integrating motion intention and impedance control in teleoperated robotic rehabilitation for upper extremity disorders". *Journal of Engineering and Science in Medical Diagnostics and Therapy,* **8**(2).

[7] Wolf, S. L., Catlin, P. A., Ellis, M., Archer, A. L., Morgan, B., and Piacentino, A., 2001. "Assessing wolf motor function test as outcome measure for research in patients after stroke". *Stroke,* **32**(7), pp. 1635–1639.

[8] Sheng, B., Chen, X., Cheng, J., Zhang, Y., Tao, J., Duan, C., et al., 2024. "A novel scoring approach for the wolf motor function test in stroke survivors using motion-sensing technology and machine learning: A preliminary study". *Computer Methods and Programs in Biomedicine,* **243**, p. 107887.

[9] Assessment, F.-M., 2018. "Automated evaluation of upper-limb motor function impairment using". *IEEE TRANSACTIONS ON NEURAL SYSTEMS AND REHABILITATION ENGINEERING,* **26**(1), p. 125.

[10] Steele, K. M., Papazian, C., and Feldner, H. A., 2020. "Muscle activity after stroke: perspectives on deploying surface electromyography in acute care". *Frontiers in neurology,* **11**, p. 576757.

[11] Zhou, Y., and et al., 2024. "Predicting upper limb motor recovery in subacute stroke patients via fnirs-measured cerebral functional responses induced by robotic training". *J. NeuroEngineering Rehabil.,* **21**(1), Dec., p. 226.

[12] Wang, C., Sivan, M., Bao, T., Li, G., and Xie, S., 2021. "3d free reaching movement prediction of upper-limb based on deep neural networks". In 2021 10th International IEEE/EMBS Conference on Neural Engineering (NER), pp. 1005–1009.

[13] Kim, J. K., Lv, Z., Park, D., and Chang, M. C., 2022. "Practical machine learning model to predict the recovery of motor function in patients with stroke". *Eur. Neurol.,* **85**(4), Mar., pp. 273–279.

[14] Lee, S.-H., Cui, J., Liu, L., Su, M.-C., Zheng, L., and Yeh, S.-C., 2021. "An evidence-based intelligent method for upper-limb motor assessment via a vr training system on stroke rehabilitation". *IEEE Access,* **9**, pp. 65871–65881.

[15] Khan, A. M., Khan, F., Dwivedi, A. K., Semwal, V. B., Martha, S., and Bijalwan, V., 2024. "Eeg-based motion intention detection for robotic rehabilitation: Evaluating classification and regression algorithms". *SN Comput. Sci.,* **5**(8), Nov., p. 1057.

[16] Choy, C. S., Cloherty, S. L., Pirogova, E., and Fang, Q., 2023. "Virtual reality assisted motor imagery for early post-stroke recovery: A review". *IEEE Rev. Biomed. Eng.,* **16**, pp. 487–498.

[17] Ploderer, B., and et al., 2016. "How therapists use visualizations of upper limb movement information from stroke patients: A qualitative study with simulated information". *JMIR Rehabil. Assist. Technol.,* **3**(2), Oct., p. e6182.

[18] Jobsis, F. F., 1977. "Noninvasive, infrared monitoring of cerebral and myocardial oxygen sufficiency and circulatory parameters". *Science,* **198**(4323), pp. 1264–1267.

[19] Raghavan, P., 2022. "Framework for the treatment of spasticity and muscle stiffness". In *Spasticity and Muscle Stiffness: Restoring Form and Function*. Springer, pp. 155–167.

[20] Ferrari, M., Mottola, L., and Quaresima, V., 2004. "Principles, techniques, and limitations of near infrared spectroscopy". *Canadian journal of applied physiology,* **29**(4), pp. 463–487.

[21] Zhou, Y., Xie, H., Li, X., Huang, W., Wu, X., Zhang, X., Dou, Z., Li, Z., Hou, W., and Chen, L., 2024. "Predicting upper limb motor recovery in subacute stroke patients via fnirs-measured cerebral functional responses induced by robotic training". *Journal of NeuroEngineering and Rehabilitation,* **21**(1), p. 226.

[22] Kim, J. K., Lv, Z., Park, D., and Chang, M. C., 2022. "Practical machine learning model to predict the recovery of motor function in patients with stroke". *European Neurology,* **85**(4), pp. 273–279.

[23] Zhao, P., Zhang, Y., Guan, H., Deng, X., and Chen, H., 2021. "Design of a single-degree-of-freedom immersive rehabilitation device for clustered upper-limb motion". *Journal of Mechanisms and Robotics,* **13**(3), p. 031006.

[24] Zhao, P., Guan, H., Zhang, Y., Chen, Y., Deng, X., and Chen, H., 2020. "Design of single-dof immersive upper limb rehabilitation system via kinematic mapping and virtual reality". In International Design Engineering Technical Conferences and Computers and Information in Engineering Conference, Vol. 83990, American Society of Mechanical Engineers, p. V010T10A038.

[25] Zimmerli, L., Jacky, M., Lünenburger, L., Riener, R., and Bolliger, M., 2013. "Virtual reality-based neurorehabilitation for motor function: A systematic review". *European Journal of Physical and Rehabilitation Medicine,* **49**(3), pp. 357–364.

[26] Lopez-Jaquero, V., Montero, F., Fernandez-Caballero, A., and Gonzalez, P., 2016. "Exergames for post-stroke rehabilitation of upper limb: A review of the literature". *Journal of Biomedical Informatics,* **64**, pp. 236–247.

[27] Pereira, F. M., Lopes, F. M., Rodrigues, J. V., and Lima, R. C., 2020. "Gamification in physical therapy: A systematic review of related applications and clinical outcomes". *Technology and Health Care,* **28**(6), pp. 663–676.